# A W-band MMIC amplifier using 70-nm gate length InP HEMT technology

Mikael Malmkvist, Anders Mellberg, and Jan Grahn

Chalmers University of Technology, MC2, Microwave Electronics Laboratory, Kemivägen 9, SE-412 96 Göteborg, Sweden, Phone +46 31 772 10 00

*Abstract* — **InP HEMT transistors using 70-nm gate length have been fabricated and modeled. Two different epitaxial structures have been tested based on either single- or composite InGaAs channel. The composite-channel HEMT exhibited significantly higher maximum transconductance, 1370 mS/mm, compared to 860 mS/mm for the single-channel HEMT whereas $f_t$ ($f_{max}$) was approximately the same, 190 (260) GHz, and 200 (320) GHz, respectively. A W-band microstrip MMIC amplifier using 70-nm gate length InP HEMT technology has been designed and fabricated for the single-channel structure. The one-stage amplifier exhibited a gain of 8 dB at 94 GHz.**

## I. INTRODUCTION

InGaAs-InAlAs-InP HEMT technology is the preferred choice for circuit applications targeting low noise at mm-wave frequencies. However, the optimization of a sub-100 nm technology is very sensitive to a number of parameters in the epitaxial structure [1]. We here report issues of design, fabrication and modeling of 70-nm gate length InP HEMTs using either a single or a composite structure in the active channel. The single-channel design has been implemented in a microstrip-based process. A one-stage W-band MMIC amplifier is demonstrated.

## II. HEMT STRUCTURES

The layers of the two different HEMT structures were grown by molecular beam epitaxy (MBE) on a Fe-doped semi-insulating InP substrate. The composite channel contains an InGaAs super-lattice structure with five periods of four-to-one monolayers InAs/GaAs resulting in an effective composition of 80% In. The gate-to-channel distance is 115 Å for the single-channel and 140 Å for the composite-channel. Details for the different layers are given in Fig. 1.

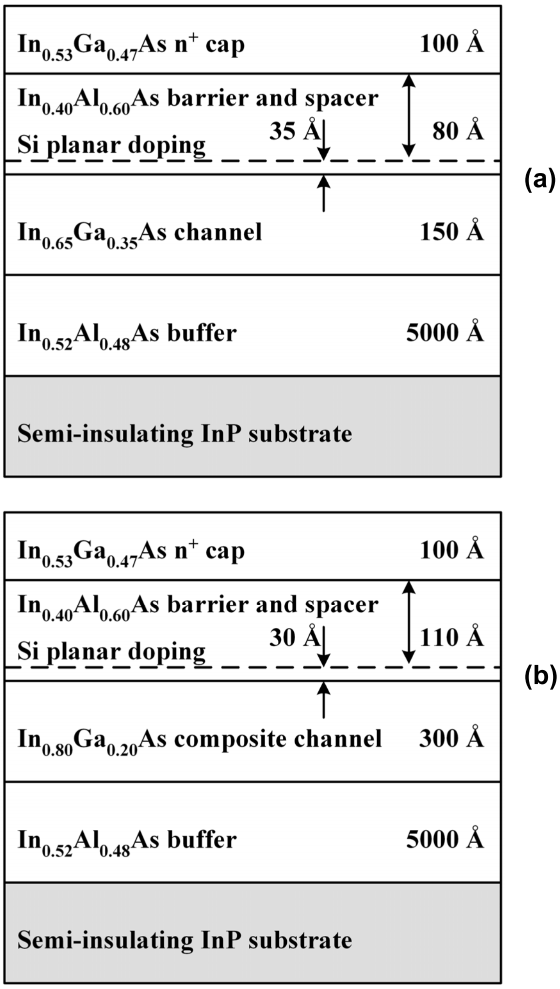

Fig. 1. Epitaxial InP HEMT structure for (a) single-channel and (b) composite-channel design.

## III. DEVICE PERFORMANCE

Details of the processing flow of the transistors are described in Ref. [2]. A scanning-electron microscope (SEM) image of a device is shown in Fig. 2. The DC current-voltage (I-V) characteristics of passivated 2x35 µm devices were measured on-wafer, see Fig. 3. The thickness of the Schottky barrier for the single-channel material was probably too low hence explaining the suppression of the drain current $I_d$. The pinch-off characteristic is well-behaved for both devices. The measured extrinsic transconductance $g_m$ is shown in Fig. 4. A maximum $g_m$ of 860 mS/mm and 1370 mS/mm is obtained for the single- and composite-channel design, respectively, at a $V_{ds}$ of 1.0 V. The difference in $g_m$ between the two channel design seen in Fig. 4 is connected to the difference in the electron mobility $\mu_n$ and sheet carrier concentration $n_s$ for the two HEMT structures; The measured $\mu_n \, x \, n_s$ is more than 50% larger for the composite-channel compared to the single channel design.

The s-parameters of the devices were measured on-wafer up to 50 GHz using coplanar probes and a HP8510

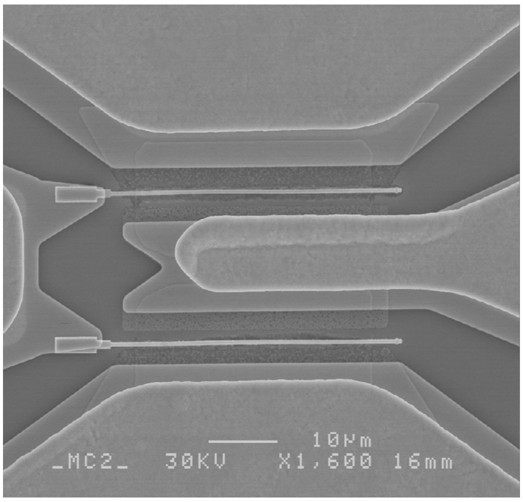

Fig. 2. A SEM image of a 70-nm InP HEMT with a gate width of 2x35 μm.

vector network analyzer. A -20 dB/decade extrapolation of current gain ($|h_{21}|^2$) and Mason's gain ($U$) versus frequency using least square fits gives an extrinsic $f_t$ and $f_{max}$ of 200 GHz and 320 GHz, respectively for the single-channel HEMT. For the composite design, $f_t$ was extrapolated to 190 GHz and $f_{max}$ to 260 GHz, see Fig. 5. Despite the large difference in $g_m$ between the two HEMTs, the $f_T$ and $f_{max}$ numbers are approximately the same. This is explained by the higher output conductance for the composite-channel design. In other words, $g_m/g_d$ is similar for the two HEMTs as verified by extracted device small-signal model parameters.

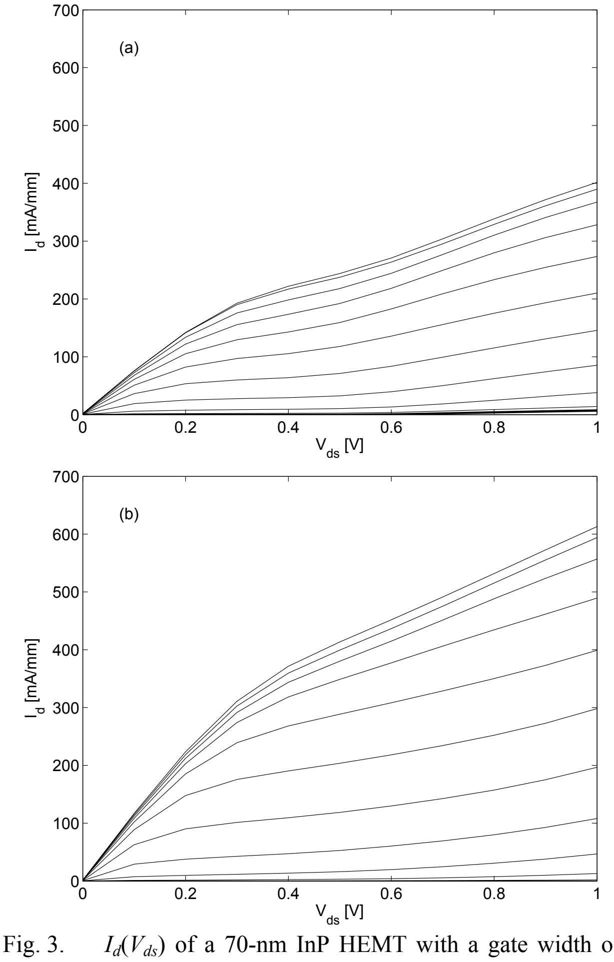

Fig. 3. $I_d(V_{ds})$ of a 70-nm InP HEMT with a gate width of 2x35 μm. $V_{gs}$: -0.6 V-0.4 V in steps of 75 mV. (a) Single-channel (b) composite-channel design.

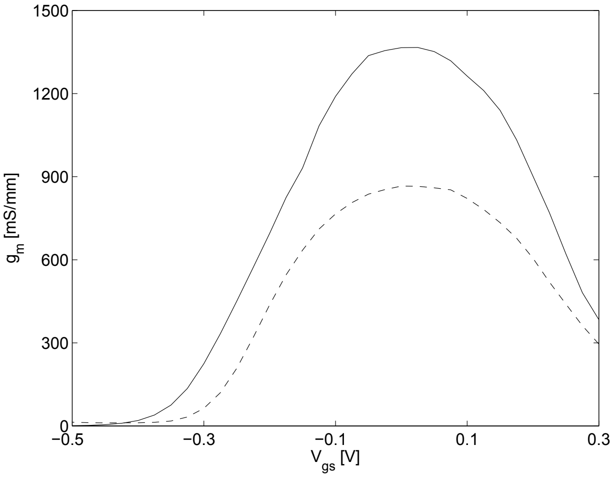

Fig. 4. $g_m(V_{gs})$ at $V_{ds}$=1.0 V of 2x35 μm gate width devices with gate lengths of 70-nm. The single-channel is the dashed line and the composite-channel is the solid line.

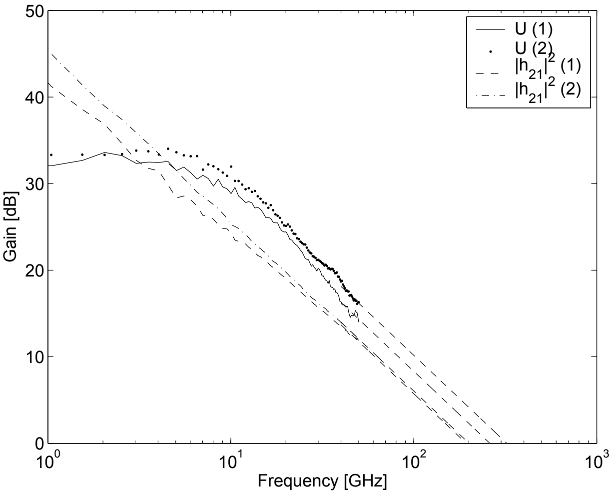

Fig. 5. Extracted current gain $|h_{21}|^2$ and unilateral power gain $U$ for the different structures at $V_{ds}$=1.1 V. (1) Composite-channel and (2) single-channel design.

## IV. DEVICE MODELING

The devices have been modeled by a direct extraction method and optimized using a sequential optimization method [3]. In Fig. 6, the small signal model used for these InP HEMT devices is shown. A normalized error analysis of the model has been performed over 168 different bias points. The normalized error function ε is defined as:

$$\varepsilon = \frac{1}{4N} \sum_{j=1}^{2} \sum_{i=1}^{2} \frac{1}{\max\left|S_{ij}^{meas}\right|^2} \sum_{k=1}^{N} \left|S_{ij}^{meas}(k) - S_{ij}^{model}(k)\right|^2 \quad (1)$$

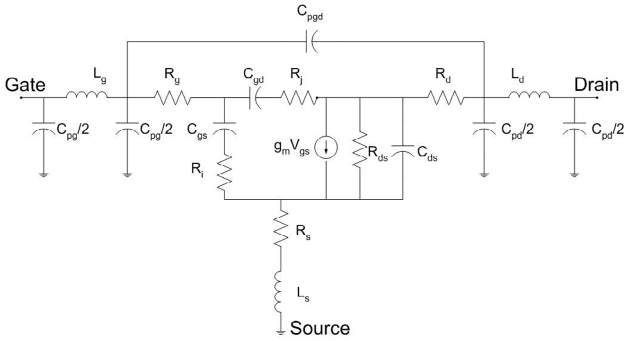

Fig. 6. InP HEMT small-signal model.

In Fig. 7 the normalized errors for the different materials are plotted versus $V_{ds}$ and $V_{gs}$. The models exhibit a good fit over a large range of bias points and can therefore be used for large signal modeling. The error increases at higher $V_{ds}$ due to impact ionization [4], which is not accounted for in the model. The variation in normalized error for the composite-channel is correlated to the bias dependence of $g_m$.

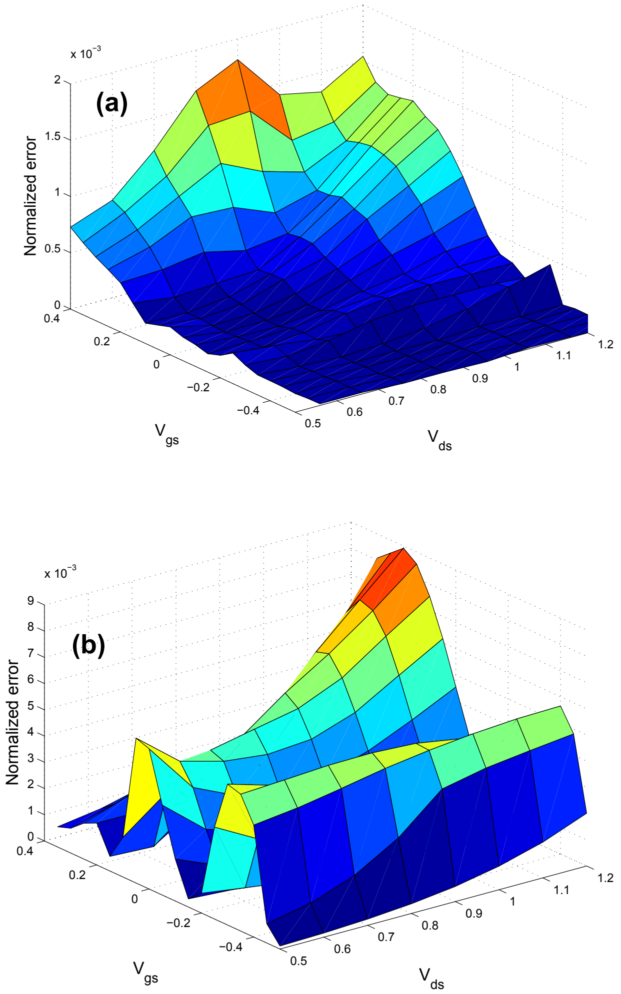

Fig. 7. Normalized error for a (a) single-channel and (b) composite channel InP HEMT at 168 different bias points.

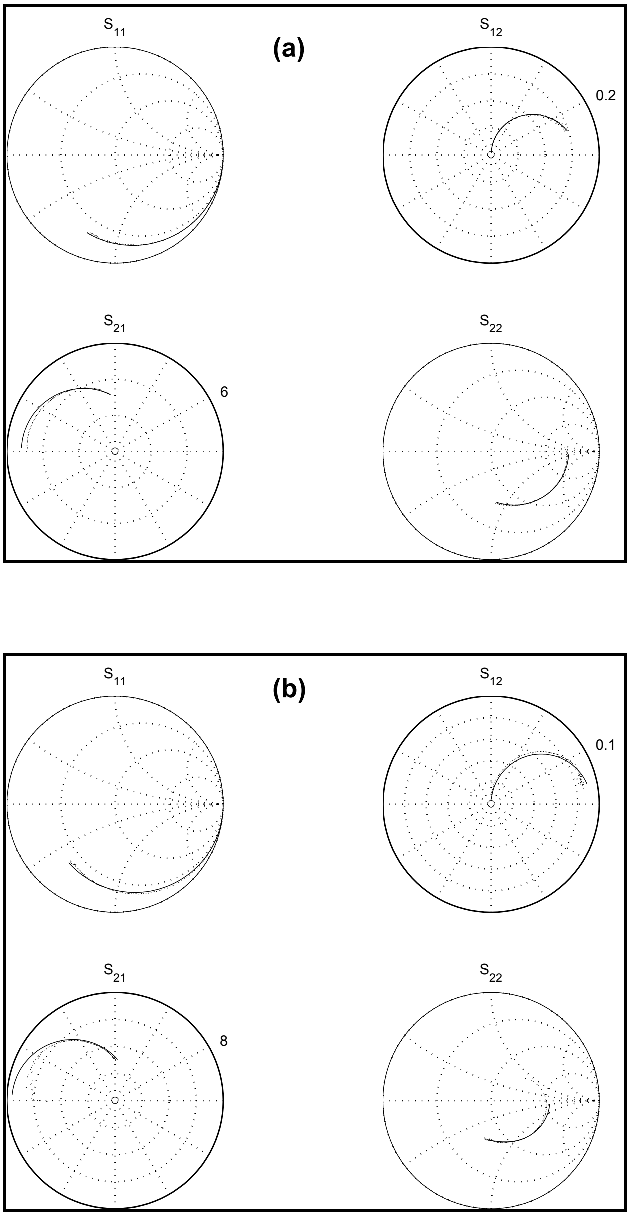

Fig. 8. Measured (dotted line) and modeled (solid line) s-parameters for the (a) single-channel ($V_{ds}$=1.1 V, $V_{gs}$=0 V) and (b) composite channel ($V_{ds}$=1.1 V, $V_{gs}$=0.15 V) InP HEMT.

Fig. 8 shows the measured and modeled s-parameters at $V_{ds}$=1.1 V between 1 GHz and 50 GHz. Apart from lower frequencies below 5 GHz, the agreement is excellent for all s-parameters. To achieve a better fit with the measured data at low frequencies, the model must include a part which describes impact ionization.

## V. MMIC PERFORMANCE

The W-band amplifier was designed using 2x35 µm InP HEMT single-channel devices. The agreement between the applied small-signal model and measured data is represented in Fig. 8(a). The model is extrapolated to W-band. The s-parameters of the amplifier were measured with a W-band test set using an on-chip TRL calibration. The transistor was biased through bias Tees. As depicted in Fig. 9, the amplifier exhibited more than 8 dB gain over 75-94 GHz.

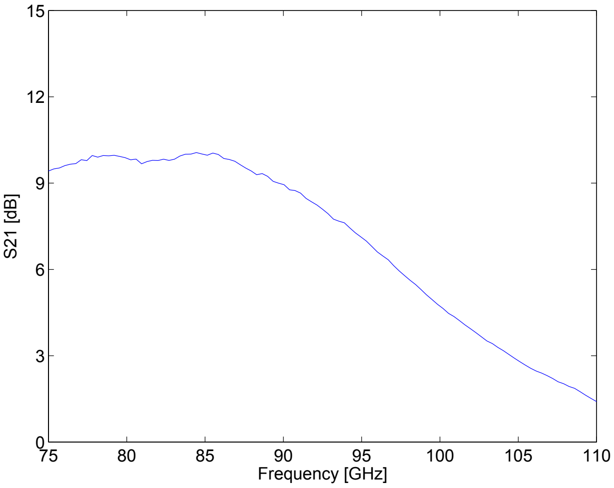

Fig. 9. Measured gain ($S_{21}$) for the W-band amplifier.

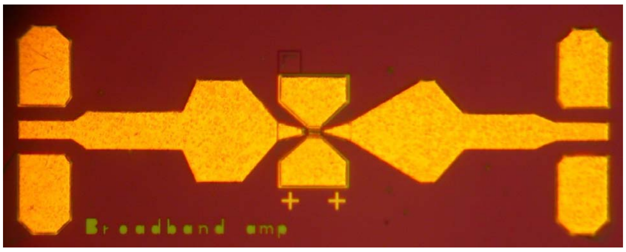

Fig. 10. Photograph of the W-band amplifier

Fig. 10 shows a picture of the fabricated one-stage amplifier.

## VI. CONCLUSION

We have investigated two different 70-nm gate length InP HEMTs based on either single- or composite InGaAs channel design. A W-band microstrip amplifier has been fabricated and characterized for the single-channel 70-nm InP HEMT. The amplifier exhibited more than 8 dB gain from 75 to 94 GHz.

## ACKNOWLEDGEMENT

Dr. Shumin Wang at Chalmers University of Technology is acknowledged for providing the epitaxial structure for one of the samples in this study. We are grateful for the support from the Swedish Research Council (VR) and the Swedish Foundation for Strategic Research (SSF) through the Strategic Research Center for High Speed Electronics and Photonics at Chalmers University of Technology.

## REFERENCES

[1] T. Parenty, S. Bollaert, J. Mateos, X. Wallart and A. Cappy, "Design and realization of sub 100nm gate length HEMTs", *13th International Conference on Indium Phosphide and Related Materials*, pp. 626-629, 2001.

[2] M. Malmkvist, A. Mellberg, J. Grahn, N. Rorsman and H. Zirath, "A 50-nm gate length InP pseudomorphic HEMT implemented in an MMIC broadband feedback amplifier", *16th International Conference on Indium Phosphide and Related Materials*, pp. 386-388, 2004.

[3] C. Niekerk, P. Meyer, D. M. M.-P. Schreurs and P. B. Winson, "A robust integrated multibias parameter-extraction method for MESFET and HEMT models", *IEEE Transactions on MTT*, Vol. 48 pp. 777-785, 2000.

[4] R. Reuter, M. Agethen, U. Auer, S. van Waasen, D. Peters, W. Brockenhoff and F. J. Tegude, "Investigation and modeling of impact ionization with regard to RF- and noise behavior of HFET" , *IEEE Transactions on MTT*, Vol. 45 pp. 977-983, 1997.